

Photoemission study of the itinerant-electron helimagnet $\text{Fe}_x\text{Co}_{1-x}\text{Si}$

J.-Y. Son, K. Okazaki, T. Mizokawa, and A. Fujimori

Department of Physics and Department of Complexity Science and Engineering, University of Tokyo, Bunkyo-ku, Tokyo 113-0033, Japan

T. Kanomata

Faculty of Engineering, Tohoku Gakuin University, Tagajo 985-8537, Japan

R. Note

Institute for Materials Research, Tohoku University, Katahira, Aoba-ku, Sendai 980-8577, Japan

(Received 5 June 2003; revised manuscript received 28 July 2003; published 24 October 2003)

$\text{Fe}_x\text{Co}_{1-x}\text{Si}$ is a metal with helical spin structure in the concentration range $0.2 < x < 0.95$ although the end members are a narrow-gap semiconductor (FeSi) and a diamagnetic semimetal (CoSi). We have studied the electronic structure of $\text{Fe}_x\text{Co}_{1-x}\text{Si}$ ($x = 0.5, 0.8$) using ultraviolet photoemission spectroscopy. With Fe substitution for Co, the structure due to the transition-metal $3d$ states is shifted toward lower binding energies, qualitatively consistent with the prediction of the rigid-band model. Although the superposition of the spectra of FeSi and CoSi better describes the x dependence of the global spectral features than the rigid-band model, the x dependence near the Fermi level (E_F) is better described by the rigid-band model. The appearance of magnetic order in $\text{Fe}_x\text{Co}_{1-x}\text{Si}$ may thus be explained by the rigid-band model, which predicts that the density of states at E_F is low or zero for CoSi and FeSi but becomes large for intermediate x . We also find a weak temperature dependence around the Fermi level, qualitatively consistent with the increase in the electrical resistivity below the Néel temperature (T_N).

DOI: 10.1103/PhysRevB.68.134447

PACS number(s): 75.30.Kz, 79.60.Bm, 71.20.Lp

I. INTRODUCTION

The solid solution of two monosilicides FeSi and CoSi—namely, $\text{Fe}_x\text{Co}_{1-x}\text{Si}$ —has attracted interest because of its unique magnetic and electrical properties.^{1–4} While FeSi is an unusual narrow-gap semiconductor and CoSi is a diamagnetic semimetal,⁵ $\text{Fe}_x\text{Co}_{1-x}\text{Si}$ exhibits a magnetically ordered phase at low temperatures in the concentration range of $0.2 \leq x \leq 0.95$.^{5,6} According to a small-angle neutron scattering experiment,^{7,8} $\text{Fe}_x\text{Co}_{1-x}\text{Si}$ with $0.3 \leq x \leq 0.9$ shows a helical spin order with a long periodicity—i.e., nearly ferromagnetic, as in the case of MnSi. Under a magnetic field, the helical spin structure is transformed to a conical one and then to the induced ferromagnetic state above a critical field H_c . Arrott plots for the same samples show a slight deviation from straight lines,⁹ in a similar way to MnSi.¹⁰ From extrapolation of the straight part of the magnetization curve to $H = 0$, the Curie temperature T_c is obtained as 44.5 and 44 K for $\text{Fe}_{0.8}\text{Co}_{0.2}\text{Si}$ and $\text{Fe}_{0.5}\text{Co}_{0.5}\text{Si}$, respectively. In order to understand those unusual magnetic properties, knowledge of the electronic structure, particularly the effect of alloying and the composition-dependence is necessary.

In this work, in order to obtain experimental information about the electronic structure of $\text{Fe}_x\text{Co}_{1-x}\text{Si}$, we have made an ultraviolet photoemission study of $\text{Fe}_x\text{Co}_{1-x}\text{Si}$ with $x = 0.5$ and 0.8 . As a reference compound, photoemission spectra of CoSi have also been measured. Recently, Susaki *et al.*¹¹ have performed a detailed photoemission study of $\text{Fe}_{1-x}\text{Co}_x\text{Si}$ with low Co concentration ($x = 0.05$ and 0.1), where the system is in the paramagnetic phase, and found that the hybridization gap in FeSi is gradually filled when a small amount ($x \sim 0.05$) of Co is substituted for Fe.

II. EXPERIMENT

Polycrystalline samples of $\text{Fe}_x\text{Co}_{1-x}\text{Si}$ with $x = 0.5$ and 0.8 and a single crystal of CoSi were prepared from 99.99%-pure Fe, 99.9%-pure Co, and 99.999%-pure Si by arc melting in an argon atmosphere. A CoSi single crystal was grown by the Czochralski technique and checked by Laue x-ray diffraction. In order to check the sample composition, we have made Fe $2p$ and Co $2p$ core-level x-ray photoemission spectroscopy (XPS). The composition of $\text{Fe}_{0.8}\text{Co}_{0.2}\text{Si}$ was found to be $\text{Fe}_{0.79}\text{Co}_{0.21}\text{Si}$.

Ultraviolet photoemission spectroscopy (UPS) measurements were carried out using a VSW CLASS-150 hemispherical analyzer or an Omicron EA-125 analyzer and a He discharge lamp (He I: $h\nu = 21.2$ eV, He II: $h\nu = 40.8$ eV). The angular resolution of the VSW and Omicron analyzer was $\pm 4.5^\circ$ and $\pm 8^\circ$, respectively. The Fermi edge of Au evaporated on the sample was measured after each series of measurements in order to accurately determine the Fermi level (E_F) and the instrumental resolution. The resolution of the He I measurements was 20–35 meV. In order to obtain clean surfaces, the samples were repeatedly scraped *in situ* with a diamond file.

III. RESULTS AND DISCUSSION

Figure 1 shows He I UPS spectra for MnSi,¹² FeSi,¹¹ $\text{Fe}_{0.8}\text{Co}_{0.2}\text{Si}$, $\text{Fe}_{0.5}\text{Co}_{0.5}\text{Si}$, and CoSi in the entire valence-band region (a) and near E_F (b). The inset shows a valence-band He I UPS spectrum (solid curve) of $\text{Fe}_{0.8}\text{Co}_{0.2}\text{Si}$ and its background (dashed curve) subtraction. Here, the background is assumed proportional to the integral of the measured spectrum. This background subtraction procedure has

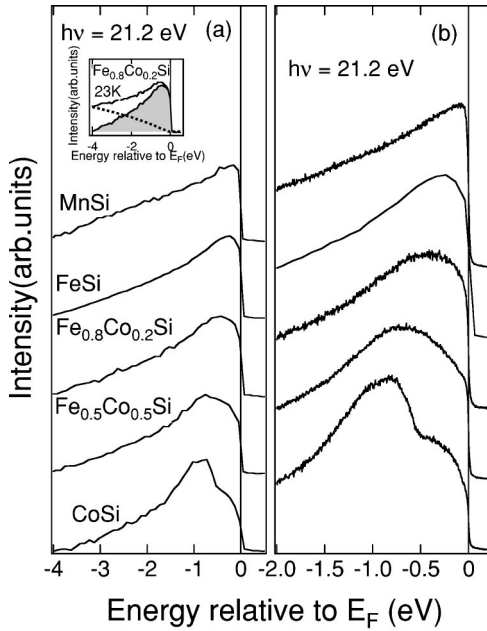


FIG. 1. Comparison of He I UPS spectra in the entire valence-band region (a) and near E_F (b) of MnSi (Ref. 12), FeSi (Ref. 11), $Fe_{0.8}Co_{0.2}Si$, $Fe_{0.5}Co_{0.5}Si$, and CoSi. The spectra have been normalized to the total area. The inset shows the spectrum (solid curve) for $Fe_{0.8}Co_{0.2}Si$ and its background (dashed curve) subtraction.

been successfully employed to describe the inelastic background when photoelectron energies are as low as in He I UPS.¹³

In general, photoemission spectra are affected by surface effects due to the short mean free paths of photoelectrons, and it is not trivial to decompose the spectra into surface and bulk components. In the present case, the kinetic energy dependence of the photoelectron mean free path can be utilized to perform such a decomposition because the photoionization cross sections of both the He I and He II spectra are dominated by the metal d partial density of states (DOS) and Si $3sp$ contributions are negligible,¹⁴ meaning that the bulk and surface spectral line shapes do not change appreciably with photon energy and that the photon-energy dependence of the spectrum is largely due to the different degrees of surface and bulk contributions between He I and He II. Therefore, we subtracted the He II spectra from the He I spectra to obtain the “bulk” spectra shown in Fig. 2. Prior to the subtraction, the He I spectra had been broadened with the He II resolution. Here, we have assumed that the surface contribution comes from the outermost atomic layer for all samples because the $Fe_xCo_{1-x}Si$ alloys have the same B20 structure at any concentration.¹⁵ Thus the surface contribution to the spectra becomes $1 - \exp(-d/\lambda)$, where λ is the electron mean free path and d is the thickness of the outermost atomic layer. We have assumed that $d = a/2$, where a is the cubic lattice constant of CoSi/FeSi because each cube contains two CoSi/FeSi molecules. Contributions from the first atomic layer for He I and He II in CoSi/FeSi thus calculated (Table I) show that the He II spectra contain a larger ($\sim 37\%$) amount of surface contributions while the He I spectra contain a smaller ($\sim 20\%$) amount of surface contributions. The

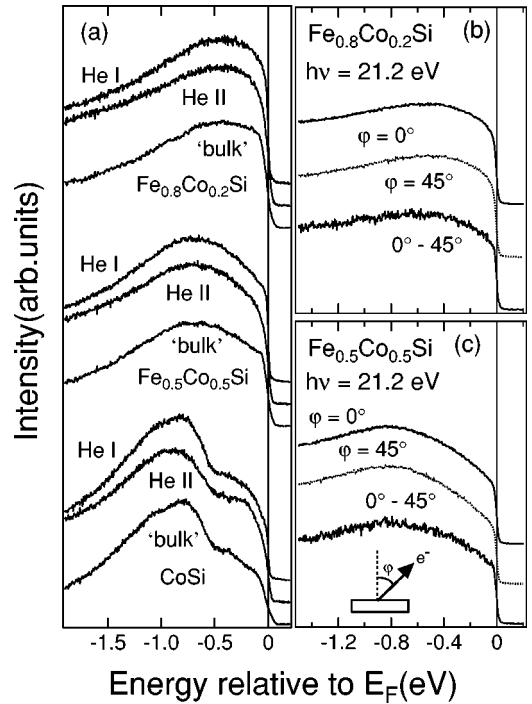


FIG. 2. He I and He II UPS spectra for $Fe_{0.8}Co_{0.2}Si$, $Fe_{0.5}Co_{0.5}Si$, and CoSi near E_F (a). The He I–He II different spectra represent “bulk” spectra. (b) and (c) show He I UPS spectra for angles 0° and 45° between the photoelectron momentum and the surface normal for $Fe_{0.8}Co_{0.2}Si$ and $Fe_{0.5}Co_{0.5}Si$. The 0° – 45° difference spectrum again represents a “bulk” spectrum. Prior to subtraction, the spectra have been normalized as described in the text.

“bulk” spectra were therefore obtained by subtracting the He II spectra (multiplied by 20/37) from the He I spectra. The “bulk” spectra thus obtained show that the structure around E_F is stronger and sharper than the raw He I and He II data except for CoSi.

In order to check the consistency of the above decomposition procedure, we have also made measurements by changing the angle between the sample surface and the analyzer, thereby changing the escape depth of photoelectrons according to $F = \lambda \cos \varphi$. The He I UPS spectra for angles 0° and 45° between the photoelectron momentum and the surface normal are shown in Figs. 2(b) and 2(c) together with a “bulk” spectrum obtained by subtracting the 45° spectrum from the 0° spectrum after an appropriate intensity normalization. The result again shows that the structure around E_F is enhanced, qualitatively consistent with the “bulk” spectrum in (a), however, the peak around E_F is somewhat weaker than in (a). This quantitative discrepancy between the

TABLE I. Contributions from the outermost surface atomic layer to the He I and He II UPS spectra of CoSi/FeSi. Here, a cubic lattice constant 2.3 \AA has been used.

Light source	Mean free path	Surface layer contribution
He I(21.2 eV)	$\sim 10 \text{ \AA}$	$\sim 20\%$
He II(40.8 eV)	$\sim 5 \text{ \AA}$	$\sim 37\%$

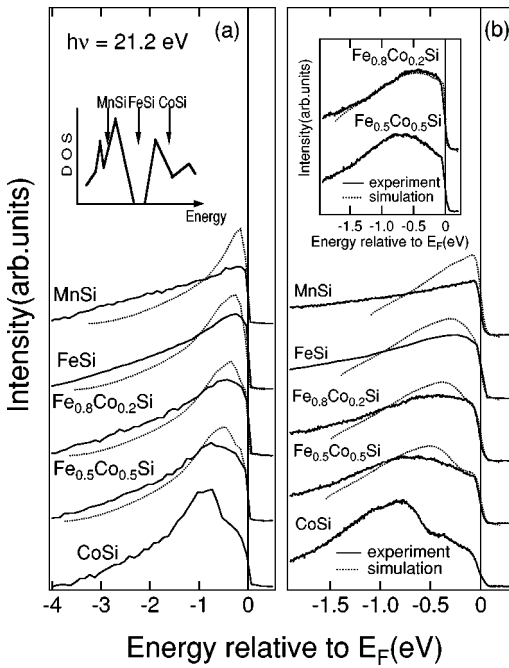


FIG. 3. Comparison of the measured “bulk” spectra [Fig. 2(a)] with the simulation assuming the rigid-band model starting from CoSi. Dotted curves show the simulated spectra. The spectra have been normalized as described in the text. The inset to (a) shows the Fermi level position in the rigid-band model for the monosilicides. The inset to (b) shows a comparison between the spectrum of $\text{Fe}_{0.8}\text{Co}_{0.2}\text{Si}$ and the simulation using the rigid-band model and the spectrum of $\text{Fe}_{0.5}\text{Co}_{0.5}\text{Si}$.

two “bulk” spectra would be attributed to the simplified assumption of the mean-free-path model employed here and the inherent roughness of the sample surfaces prepared by scraping. Thus we can conclude that, although the difference between the “bulk” spectra and He I UPS spectra is finite, it is not large and that conclusions from the following discussions will not be altered by the surface effects.

Now, let us examine the alloying effect on the electronic structure of $\text{Fe}_x\text{Co}_{1-x}\text{Si}$ based on the photoemission spectra. The structure at ~ -0.8 eV in CoSi is shifted toward lower binding energy with increasing Fe concentration. According to band-structure calculations, the Fermi level in MnSi is located within the band below the gap,¹⁶ it is located within the gap in FeSi, and it is located in the band above the gap in CoSi (Ref. 17) as shown in the inset of Fig. 3(a). This means that, as the number of 3d electrons increases, the Fermi level is shifted upward and moves across the energy gap. Indeed, the UPS spectra of CoSi show a dip structure at ~ -0.5 eV, where the band-structure calculation predicts the band gap.¹⁷ Therefore, we have attempted to simulate the x dependence of the spectra of $\text{Fe}_x\text{Co}_{1-x}\text{Si}$ within the simplest rigid-band model. To do this, we have utilized the facts that the photoionization cross sections of both the He I and He II spectra are dominated by the metal d partial DOS and that Si 3sp contributions are negligibly small. Starting from the spectra of CoSi, E_F were shifted downward so that the integrated area below E_F was proportional to the number of 3d electrons n_d . We have assumed that $n_d = 5, 6, 6.2, 6.5,$ and 7

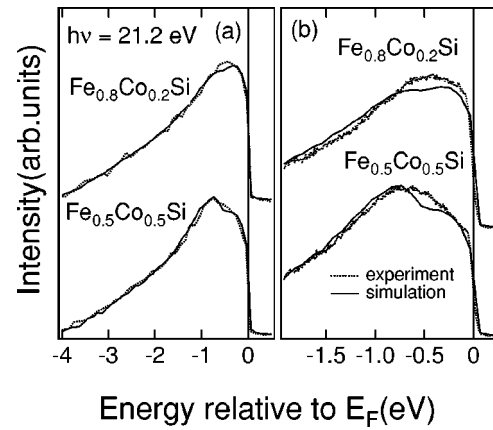


FIG. 4. Comparison of the measured “bulk” spectra of $\text{Fe}_{0.8}\text{Co}_{0.2}\text{Si}$ and $\text{Fe}_{0.5}\text{Co}_{0.5}\text{Si}$ with the superpositions of the spectra of FeSi and CoSi.

for MnSi, FeSi, $\text{Fe}_{0.8}\text{Co}_{0.2}\text{Si}$, $\text{Fe}_{0.5}\text{Co}_{0.5}\text{Si}$, and CoSi, respectively, the same as the d -electron numbers of the free atoms. The result is shown in Fig. 3, where the integrated areas of the measured spectra have also been normalized to the above n_d 's. The figure shows that the simulated spectra are in quali-

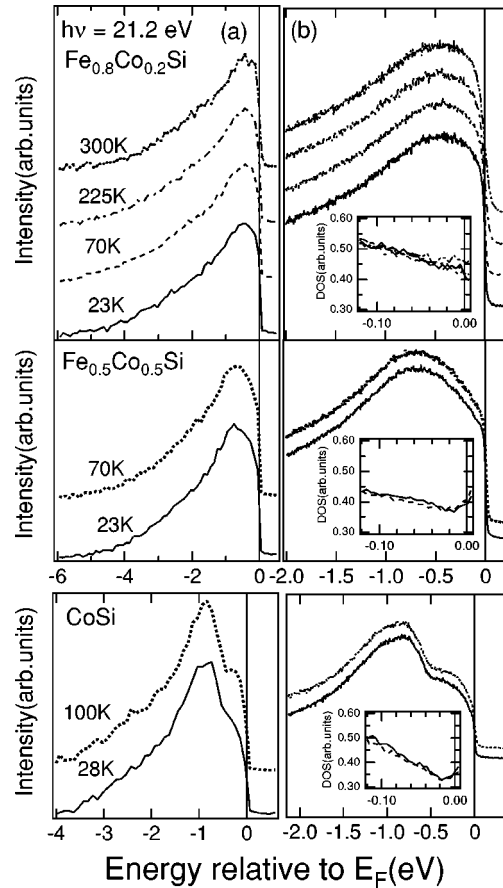


FIG. 5. He I UPS spectra of $\text{Fe}_{0.8}\text{Co}_{0.2}\text{Si}$, $\text{Fe}_{0.5}\text{Co}_{0.5}\text{Si}$, and CoSi in the entire valence-band region (a) and near E_F (b) at various temperatures. The spectra have been normalized to the total area. The inset shows the temperature-dependent spectra in the vicinity of E_F divided by the Fermi-Dirac distribution function.

tative agreement with the measured spectra although the measured spectra tend to be broader than the simulated spectra as n_d decreases, which suggests that electron correlation becomes stronger in the series $\text{CoSi} \rightarrow \text{FeSi} \rightarrow \text{MnSi}$.

As an alternative way to see the effect of alloying in $\text{Fe}_x\text{Co}_{1-x}\text{Si}$, we have simulated the spectra for $\text{Fe}_x\text{Co}_{1-x}\text{Si}$ by superposing the spectra of FeSi and CoSi. In this simulation, the spectrum of $\text{Fe}_x\text{Co}_{1-x}\text{Si}$, $\rho_x(\omega)$, is given by $[x\rho_{\text{FeSi}}(\omega)\sigma_d(\text{Fe}) + (1-x)\rho_{\text{CoSi}}(\omega)\sigma_d(\text{Co})]/[x\sigma_d(\text{Fe}) + (1-x)\sigma_d(\text{Co})]$, where $\rho_{\text{FeSi}}(\omega)$ and $\rho_{\text{CoSi}}(\omega)$ are the measured spectra of FeSi and CoSi and $\sigma_d(\text{Fe})$ and $\sigma_d(\text{Co})$ are the atomic cross sections of Fe $3d$ and Co $3d$, respectively. As shown in Fig. 4, agreement between the measured spectra and the simulated ones is rather good. Especially, the agreement in the wide range spectra [Fig. 4(a)] is much more satisfactory than for the rigid-band model (Fig. 3). Near the Fermi level [Fig. 4(b)], however, there are some discrepancies between the superposition simulation and the experiment spectra. As shown in the inset of Fig. 3(b), the rigid-band model better describe the spectrum of $\text{Fe}_{0.8}\text{Co}_{0.2}\text{Si}$ starting from the spectrum of $\text{Fe}_{0.5}\text{Co}_{0.5}\text{Si}$. If the rigid-band model is appropriate to describe the electronic structure near E_F , it would also predict that the DOS increases for intermediate x . This will explain why $\text{Fe}_x\text{Co}_{1-x}\text{Si}$ becomes nearly ferromagnetic for intermediate x in the framework of the Stoner model.

Finally, Fig. 5 shows the temperature dependence of the He I UPS spectra in the entire valence-band region (a) and near E_F (b) for $\text{Fe}_{0.8}\text{Co}_{0.2}\text{Si}$, $\text{Fe}_{0.5}\text{Co}_{0.5}\text{Si}$, and CoSi. In the entire valence band, the measured spectra do not change with temperature on this energy scale. In order to detect subtle changes in the DOS near E_F , it is desirable to remove the effect of the temperature-dependent Fermi-Dirac distribution function. Therefore, we have divided the photoemission spectra by the Fermi-Dirac distribution function (convoluted with a Gaussian corresponding to the instrumental resolu-

tion) at each temperature. As shown in the inset of Fig. 5, the spectral DOS thus obtained for $\text{Fe}_{0.8}\text{Co}_{0.2}\text{Si}$ and $\text{Fe}_{0.5}\text{Co}_{0.5}\text{Si}$ show small changes in the spectral DOS in the vicinity of E_F . This would correspond to the increase of the electrical resistivity below T_N .⁸ The change in the DOS at E_F with temperature for $\text{Fe}_{0.8}\text{Co}_{0.2}\text{Si}$ is the largest which is also consistent with the electrical resistivity data.⁸ In the case of MnSi and FeSi, Son *et al.*¹² and Susakiet *al.*¹¹, respectively, found that the spectral DOS in the vicinity of E_F slightly decreases with decreasing temperature. The spectra of CoSi, which does not show magnetic transition, indeed show no temperature dependence around E_F .

IV. SUMMARY

We have studied the electronic structure of $\text{Fe}_x\text{Co}_{1-x}\text{Si}$ with $x=0.5$ and 0.8 by means of UPS. As we compared the spectra for MnSi,¹² FeSi,¹¹ $\text{Fe}_{0.8}\text{Co}_{0.2}\text{Si}$, $\text{Fe}_{0.5}\text{Co}_{0.5}\text{Si}$, and CoSi, the structure due to transition-metal $3d$ states at ~ -0.8 eV in CoSi is shifted toward lower binding energies with Fe substitution. Such a shift of the spectral features is qualitatively consistent with the prediction of the rigid-band model. However, in wide-range spectra, superposition of the spectra of FeSi and CoSi better describes the x -dependent behavior than the rigid-band model. Nevertheless, spectra in the vicinity of E_F are again well described by the rigid-band model. This is consistent with the increases of the DOS for intermediate x , which explains the nearly ferromagnetic behavior of $\text{Fe}_x\text{Co}_{1-x}\text{Si}$. In $\text{Fe}_{0.8}\text{Co}_{0.2}\text{Si}$ and $\text{Fe}_{0.5}\text{Co}_{0.5}\text{Si}$, the spectral weight near E_F somewhat decreases with decreasing temperature, which is consistent with the temperature dependence of the resistivity caused by magnetic ordering.

ACKNOWLEDGMENTS

We would like to thank H. Ishii and T. Susaki for technical support.

- ¹S. Asanabe, D. Shinoda, and Y. Sasaki, *Phys. Rev.* **134**, A774 (1964).
- ²V. Jaccarino, G.K. Wertheim, J.H. Wernick, L.R. Walker, and Sigurd Aarj, *Phys. Rev.* **160**, 476 (1967).
- ³H. Yasuoka, R.C. Sherwood, J.H. Wernick, and G.K. Wertheim, *Mater. Res. Bull.* **9**, 223 (1974).
- ⁴G.K. Wertheim, J.H. Wernick, and D.N.E. Buchanan, *J. Appl. Phys.* **37**, 3333 (1964).
- ⁵J.H. Wernick, G.K. Wertheim, and R.C. Sherwood, *Mater. Res. Bull.* **7**, 1431 (1972).
- ⁶D. Shinoda, *Phys. Status Solidi A* **11**, 129 (1972).
- ⁷J. Beille, J. Voiron, F. Towfiq, M. Roth, and Z.Y. Zhang, *J. Phys. F: Met. Phys.* **11**, 2153 (1981).
- ⁸J. Beille, J. Voiron, and M. Roth, *Solid State Commun.* **47**, 399 (1983).
- ⁹H. Watanabe, Y. Tazuke, and H. Nakajima, *J. Phys. Soc. Jpn.* **54**, 3978 (1985).
- ¹⁰D. Bloch, J. Voiron, V. Jaccarino, and J.H. Wernick, *Phys. Lett.*

51A, 362 (1975).

- ¹¹T. Susaki, T. Mizokawa, A. Fujimori, A. Ohno, T. Tonogai, and H. Takagi, *Phys. Rev. B* **58**, 1197 (1998).
- ¹²J.-Y. Son, K. Okazaki, T. Mizokawa, A. Fujimori, T. Kanomata, and R. Note, *J. Phys. Soc. Jpn.* **71**, 1728 (2002).
- ¹³X. Li, Z. Zhang, and V.E. Henrich, *J. Electron Spectrosc. Relat. Phenom.* **63**, 253 (1993).
- ¹⁴J.J. Yeh and I. Lindau, *At. Data Nucl. Data Tables* **32**, 1 (1985).
- ¹⁵H. Watanabe, H. Yamamoto, and K. Ito, *J. Phys. Soc. Jpn.* **18**, 995 (1963).
- ¹⁶O. Nakanishi, A. Yanase, and M. Kataoka, in *Electron Correlation and Magnetism in Narrow-Band Systems*, edited by T. Moriya, Springer Series in Solid-State Sciences, Vol. 29 (Springer-Verlag, Heidelberg, 1981), p. 126.
- ¹⁷H. Yamada, K. Terao, H. Ohta, T. Arioka, and E. Kulatov, in *Proceedings of 4th International Symposium on Advanced Physical Fields* (Tsukuba, 1999), p. 151.